IJE TRANSACTIONS B: Applications Vol. 31, No. 8, (August 2018) 1274-1282

International Journal of Engineering

Journal Homepage: www.ije.ir

Transient Entropy Generation Analysis During Wustite Pellet Reduction to Sponge Iron

A. Zare Ghadi, M. S. Valipour*, M. Biglari

Faculty of Mechanical Engineering, Semnan University, Semnan, Iran

PAPER INFO

Paper history:
Received 28 July 2017
Received in revised form 01 December 2017
Accepted 23 January 2018

Keywords:
Wustite Pellet
Entropy Generation
Mathematical Model
Grain Model

ABSTRACT

The present study carefully examined entropy generation during wustite pellet reduction to sponge iron. The finite volume method was used to solve the governing equations. The grain model was used to simulate the reaction rate. The reactant gases including carbon monoxide and hydrogen were converted to water and carbon dioxide after wustite reduction. Entropy is generated by heat transfer, mass transfer and chemical reactions. The rate of entropy generation is studied over a period of 150 minutes. Based on the governing equations, the share of each process in the generation of entropy was calculated. The effects of gas ratio, porosity, and tortuosity and grain diameter of wustite pellet on entropy generation were investigated. The porosity was changed from 0.2 to 0.5, tortuosity from 1 to 4, grain diameter from 7 to 20 mm and the ratio of reducing gas from 0.5 to 2. According to the results maximum value of entropy generation nearly occurs during first 20 minutes of the reduction process. It is shown that the heat transfer had the highest contribution to entropy generation. The results also indicates porosity and gas ratio are inversely proportional to the rate of entropy generation while tortuosity and grain diameter are directly proportional to entropy generation rate.

***doi**: 10.5829/ije.2018.31.08b.16*

NOMENCLATURE

C	Concentration	P_b	Bulk flow pressure
C_p	Specific heat at constant pressure	R_0	Pellet diameter
D	Diffusion coefficient	$\overline{R}$	Universal gas constant
d_p	Pellet diameter	R	Rate of chemical reaction
F	Local fractional reduction degree	r_g, r_c	Radii of a grain
G	Gibbs energy	$\dot{S}_h, \dot{S}_m, \dot{S}_c, \dot{S}_r$	Entropy Generation due heat transfer, mass transfer, coupling between heat and mass transfer, chemical reaction
H_2/CO	Adsorption coefficient	$\dot{S}_T$	Total entropy generation
ΔH	Heat of Reaction	t	Time
h	Effective heat transfer coefficient	T, T_b, T^0	Temperature, bulk & initial temperature
K_0	Reaction rate constant	v	Volume of pellet
K_e	Equilibrium constant	X	Overall fractional reduction degree
k_m	Mass transfer coefficient	y^0, y^s, y^b	Initial, surface & bulk mole fraction of gases

Greek Symbols		**Subscripts**	
ε	Porosity of pellet	i	Refers to gas component
τ	Tortuosity of pellet	eff	Effective parameter
ρ_s	Mass Density	b	Refers to bulk flow
μ	Chemical Potential		

*Corresponding Author's Email: msvalipur@semnan.ac.ir (M. S.Valipour)

Please cite this article as: A. Zare Ghadi, M. S. Valipour, M. Biglari, Transient Entropy Generation Analysis During Wustite Pellet Reduction to Sponge Iron, International Journal of Engineering (IJE), IJE TRANSACTIONS B: Applications Vol. 31, No. 8, (August 2018) 1274-1282

1. INTRODUCTION

Wustite is an important intermediate product in MIDREX direct reduction technology and is converted to sponge iron in the final stage. Iron oxide (hematite) is usually reduced in three stages including reduction of hematite to magnetite, magnetite to wustite and wustite to sponge iron. Among them, wustite reduction to iron is the slowest step and controls the rate of reduction reactions [1]. Accordingly, comprehensive knowledge of wustite reduction to iron could be an important step in understanding the performance of direct reduction furnaces. Based on this knowledge, the performance of direct reduction furnaces can be improved. Consequently a number of empirical and numerical investigations have been carried out to examine the reduction process of a commercial pellet including von Bogdandy [2], McKewan [3], Turkdogan [4] and Usui et al. [5]. Some of the mentioned researches assumed rather simple formulations such as pseudosteady state, isothermal and single reactant. Some of the studies have been carried out for isothermal steady state reduction process either with pure hydrogen. Later, Valipour and Khoshandam [6] reported a significant study in which they eliminated most limitations of the previous works and studied time-dependent, non-isothermal reduction of wustite pellet with syngas. Recently, Ghadi et al. [7] investigated the capability of grain model to simulate wustite pellet reduction. They found that grain model, unlike the unreacted shrinking core model, can appropriately predict the effect of gas mixture parameters and pellet characteristics on the reduction degree. Ghadi et al. [8] also scrutinized heat and mass distribution through the wustite pellet and found their relation to reduction degree.

Despite much experimental and numerical research on wustite reduction, there is no study on entropy generation during the reduction process. Clearly, high reversible processes of heat transfer, mass transfer and chemical reactions occur simultaneously during the reduction. All these processes increase the entropy and reduce exergy (available energy or useful work generated by the system). Therefore, entropy generation should be reduced as much as possible to minimize exergy losses and to achieve the maximum usable energy. This shows the importance of entropy generation in the reduction process. To investigate this issue, the sources of entropy generation should be accurately identified to determine their contribution in entropy generation.

The aim of the present study is to investigate transient entropy generation during wustite pellet reduction to sponge iron. Grain model was used to simulate the reduction rate [9, 10] and the governing equations were given with some assumptions which are considerably simplify solution of the equations. The numerical methods used to solve the equations and entropy generation calculations are given in the relevant sections. The effects of gas ratio, grain size, porosity and tortuosity on the rate of entropy generation were studied.

2. PROBLEM DESCRIPTION

The spherical wustite sample is a porous sphere which reacts with hydrogen and carbon monoxide according to the following reactions [6]:

$$FeO + CO \rightarrow Fe + CO_2 \quad (1)$$

$$FeO + H_2 \rightarrow Fe + H_2O \quad (2)$$

The chemical reaction occurs on iron-wustite interface in all directions and progresses with time to convert all wustite to sponge iron. The wustite pellet is composed of many small spherical grains and the gas mixture reaches the outer surface of grains through the pores of wustite pellet. The reaction takes place within the spherical wustite and on the surfaces of small grains. The grains close to the outer surface are reduced faster and those closer to the center are reduced over a longer period to be converted into iron. The well-known grain model has been studied by many researchers and a good agreement with experimental results was observed [10]. The schematic model is shown in Figure 1.

The basic assumptions in the model used to derive the governing equations are given. It should be noted that these assumptions do not change the physics of the problem. As can be seen, the results have a good agreement with experimental results. Assumptions are stated as follows:

- The porosity of wustite pellet is assumed to be constant during the reduction process. The spherical particle is composed of a large number of spherical solid grains.
- Reduction is irreversible and its rate is controlled by reactions between gaseous species and diffusion of gases.
- The grain size does not change with the progress of reaction and no cracks (or shrinkage) are formed.
- The total pressure in the solution domain is constant during the reduction process.
- Gas-water shift reaction is neglected [1].

2. 1. Governing Equations Based on the above assumptions, heat and mass transfer and the reduction rates are as follows:

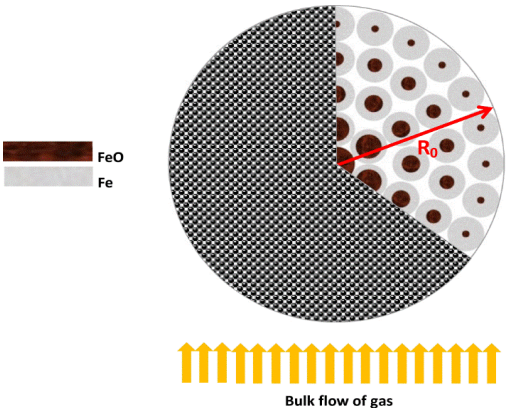

Figure 1. Sketch of reduction mechanism in pellet

a) Heat Transfer Equations

$$(\rho C_p)_{eff}\frac{\partial T}{\partial t}=\nabla(k_{eff}\nabla T)+(1-\varepsilon)\sum_{j=CO,H_2}(-R_j)\Delta H_j \quad (3)$$

b) Mass Transfer Equations

$$\frac{\partial(\varepsilon y_j)}{\partial t}=\nabla.(D_{eff,j}\nabla y_j)+(1-\varepsilon)R_j \qquad j=CO,H_2 \quad (4)$$

The reaction rate is calculated according to the following equation:

$$R_{H_2}=\frac{3K_{0,H_2}}{r_g}\left(1+\frac{1}{Ke_{H_2}}\right)(1-f)^{2/3}(Y_{H_2}) \quad (5)$$

$$R_{CO}=\frac{3K_{0,CO}}{r_g}\left(1+\frac{1}{Ke_{CO}}\right)(1-f)^{2/3}(Y_{CO}) \quad (6)$$

The local reduction rate can be calculated using the following equation:

$$\frac{\partial f}{\partial t}=\sum\left(\frac{3K_{0,j}}{\rho r_g}\right)\left(1+\frac{1}{Ke_j}\right)(1-f)^{2/3}(C_j-C_{j,e}) \quad (7)$$

The derivation of all equations with initial and boundary conditions and an estimate of the required quantities are fully discussed in the literature [10].

2. 2. Entropy Generation Formulation The rate of local entropy generation per unit volume in a continuous environment which involves the transfer of energy and mass as well as chemical reactions is discussed as follows [11-23]:

$$\dot{S}_T=\dot{S}_h+\dot{S}_m+\dot{S}_c+\dot{S}_r \quad (8)$$

where, $\dot{S}_T$ is the total rate of entropy generated by various processes. The terms on the right side of the above equation represent entropy generation rate due to heat transfer [12-19, 24] and mass transfer, coupling between heat and mass transfer [20-23] and chemical reaction [21-23]. These relations can be expressed by temperature, mole fraction of gas species, reaction rate and temperature- and concentration-dependent thermo-physical properties. These terms have been extended as follows:

$$\dot{S}_h=\frac{k_{eff}}{T^2}\left(\frac{\partial T}{\partial r}\right)^2 \quad (9)$$

$$\dot{S}_m=\bar{R}\sum_i\frac{\rho D_{eff,i}}{Y_i}\left(\frac{\partial Y_i}{\partial r}\right)^2 \quad (10)$$

$$\dot{S}_c=\frac{\bar{R}}{T}\sum_i\frac{\rho D_{eff,i}}{Y_i M_i}\left(\frac{\partial Y_i}{\partial r}\frac{\partial T}{\partial r}\right) \quad (11)$$

$$\dot{S}_r=\frac{-V_g}{T}\sum_i\mu_i n_{g,i} \quad (12)$$

The rate of entropy generation per unit volume of wustite pellet is calculated as follows [20, 21]:

$$\dot{S}_T=4\pi\sum_j\int_0^{R_0}\dot{S}_j r^2 dr \qquad (j=h,m,c,r) \quad (13)$$

2. 3. Additional Equations The mass density of the gas mixture in the above equations shown can be calculated as follows:

$$\rho=\frac{M_i P}{\bar{R}T} \quad (14)$$

The chemical potential of the ideal gas is determined by the following equation:

$$\mu_i(T,P_i)=G_i(T,P_i)+\int_p^{p_i}\frac{\bar{R}T}{P}dp \quad (15)$$

After some calculation the final equation is as follows:

$$\mu_i(T,P_i)=G_i(T,P_i)+\bar{R}T\ln(Y_i) \quad (16)$$

where,G_i is the molar Gibbs energy of the gas species. A comperehensive study on chemical potential and its relations to other parameters can be found in the literature [24].

2. 4. Boundary and Initial Conditions

a) Boundary Conditions

With regard to Figure 1, at the outer surface of the pellet and t>0:

$$-D_{eff,i}\frac{\partial y_i(R_0,t)}{\partial r}=k_{m,i}(y_i(R_0,t)-y_{b,i}) \quad (17)$$

$$-\lambda_{eff}\frac{\partial T(R_0,t)}{\partial r}=h(T(R_0,t)-T_b) \quad (T_b=1000\ K) \quad (18)$$

$$f(R_0,t)=1 \tag{19}$$

Due to spherical symmetry, at the center of the pellet and t>0:

$$\frac{\partial y_i(0,t)}{\partial r}=0 \tag{20}$$

$$\frac{\partial T(0,t)}{\partial r}=0 \tag{21}$$

$$\frac{\partial f(0,t)}{\partial r}=0 \tag{22}$$

b) Initial Conditions

Initial values of time-dependent variables are defined as follows:

$$y_i(r,0)=y_i^0 \qquad 0<r<R_0 \tag{23}$$

$$T(r,0)=T^0 \qquad 0<r<R_0 \qquad (T^0=300\ K) \tag{24}$$

$$f(r,0)=0 \qquad 0<r<R_0 \tag{25}$$

3. NUMERICAL TECHNIQUE

The governing equations and boundary conditions stated in previous section are discretized according to FVM method. The governing equations are integrated over a staggered grid system. The algebraic system resulting from numerical discretization is solved by Tridiagonal Matrix Algorithm (TDMA) applied in a line going through all volumes in the computational domain [25].

To check the convergence of the iterative solution, the relative differences of the variables between two successive iterations were calculated in each time step. When this value is less than the convergence criterion, which was chosen as 10^{-6} in present work, convergence is achieved.

To eliminate the impact of grid size, grid independence study was carried out with grid numbers of 50, 70, 100, 120. It was seen that grid number of 100 is proper value for the actual size of pellet which is usually implemented in the commercial shaft furnace (6 mm <d_p < 20 mm) [10].

3. 1. Code Validation The present numerical solution is tested by likening the results of developed code with experimental data [5]. Usui et al. [5] reported experimental data of reduction of wustite pellet at hydrogen and water vapor atmosphere with temperature of 1173 K. As Figure 2 displays, the overall reduction degree calculated by our numerical procedure is excellently compatible with reported data.

4. RESULTS AND DUSCUSSION

This study estimated time-dependent entropy generation during wustite pellet reduction to sponge iron. Entropy is generated by heat and mass transfer and chemical reaction. Each process is separately evaluated to determine their contribution to entropy generation. The parameters affecting wustite reduction and therefore the rate of entropy generation include grain diameter, the ratio of reducing gases,porosity and tortuosity of wustite pellet.The rate of entropy generation was investigated over a period of 150 min. The porosity was changed from 0.2 to 0.5, tortuosity from 1 to 4, grain diameter from 7 to 20 mm and the ratio of reducing gase from 0.5 to 2.

Figure 3 shows the rate of entropy generation versus time for different porosities and various mechanisms of entropy generation. Figure 3a shows the rate of entropy generation by heat transfer versus time. As can be seen, the rate of entropy generation is sharply decreased from its maximum value and reaches value inless than 5 min. In primarily stages, there is a maximum temperature gradient due to the large difference in the temperatures of wustite pellet and the bulk flow. As a result, the rate of entropy generation is high. As the temperature of wustite pellet approaches that of the bulk flow, the rate of entropy generation is reduced. Almost in the first 5 min, the pellet temperature approaches that of the bulk flow leading to a sharp decrease in entropy generation.Then, the rate of entropy generation becomes constant for even up to 150 min. Although the reduction of wustite pellet is completed almost after 30 min, the temperature gradient (temperature difference between the surface and center of the wustite pellet) exists leading to entropy generation. On the other hand, porosity has a significant impact on the rate of thermal entropy generation.

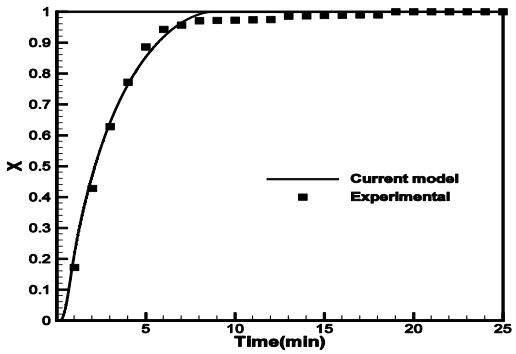

Figure 2. Comparison of model with experimental measurement from Usui et al.[5]: $Y^b_{H_2}=0.55$, $Y^b_{H_2o}=0.45$ $\varepsilon=0.4$, $\tau=4.5$, $T_b=1173\ K$, $d_p=13\ mm$

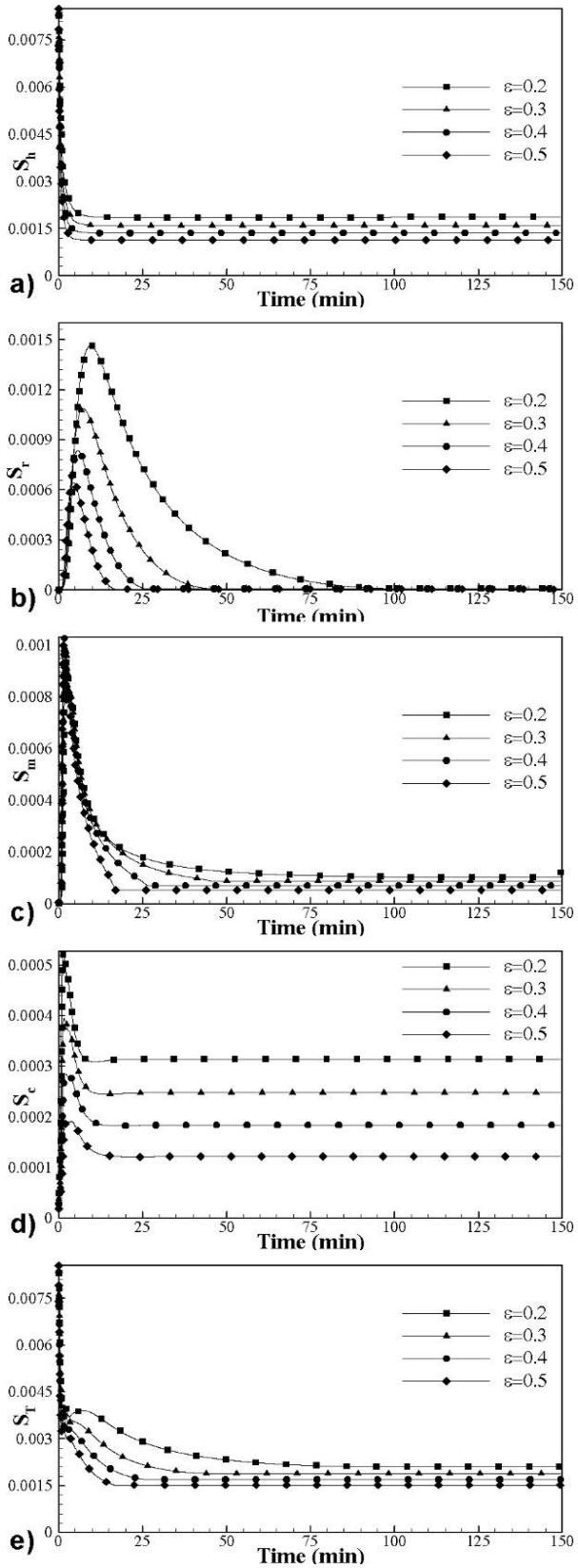

Figure 3. Entropy generation rate for different porosities (at $\tau = 2, d_p = 0.01mm, GR = 1$)

With increasing porosity, gases pass through the pores more easily because of low resistance against gas penetration. Therefore, the temperature gradient is reduced leading to a smaller temperature difference between the bulk flow and the wustite pellet. As a result, the rate of entropy generation decreases. This is clearly seen in Figure 3a. Figure 3 b shows the rate of entropy generation by chemical reactions. As can be seen, entropy generation reaches its maximum value after about 10 min and then decreases. Finally, all reducing gases are oxidized and entropy generation by chemical reaction is stopped. With increasing porosity, the maximum entropy decreases and reaches zero more quickly.

Figure 3c shows the rate of entropy generation by mass transfer. As shown, entropy increases from zero to its maximum value in early stages of reduction process and then sharply decreases and reaches a constant value. The maximum entropy at this point indicates a large mass gradient. According to Valipour [26], the molar fraction of reducing gases in this region is drastically reduced due to the complex interaction of heat and mass transfer and heat and mass-dependent chemical reactions and then increases with a moderate slope leading to this behavior of entropy generation. As can be seen in Figure 3c, entropy generation approaches zero faster with increased porosity due to reduced resistance against gas permeation. Despite complete wustite reduction to iron, entropy is not zero because of a mass gradient between the surface and center of wustite pellet caused by the solid matrix leading to entropy generation. Entropy generation due to coupling between heat and mass transfer is shown in Figure 3d. As shown, there is a peak and then entropy generation reaches a constant value but does not approach zero. As can be seen, entropy generation decreases with increasing porosity. According to Figures 3a-3d, heat transfer has the highest contribution to entropy generation and after it, chemical reaction, mass transfer and coupling between heat and mass transfer have a specific contribution to entropy generation. Figure 3e shows the rate of total entropy generation by four mechanisms. Given the share of each mechanism, the total entropy is first sharply decreased and experiences a peak and finally reaches a constant value with a moderate slope. The rate of total entropy generation decreases with increasing porosity.

The following figures show the rate of entropy generation versus time similar to what was described in the previous section. In the next section, the impact of various parameters on the rate of entropy generation is discussed and additional discussion on the behavior of samples versus time is avoided.

Figure 4 shows the rate of entropy generation versus time for different tortuosities and various mechanisms of entropy generation. Figure 4a shows the

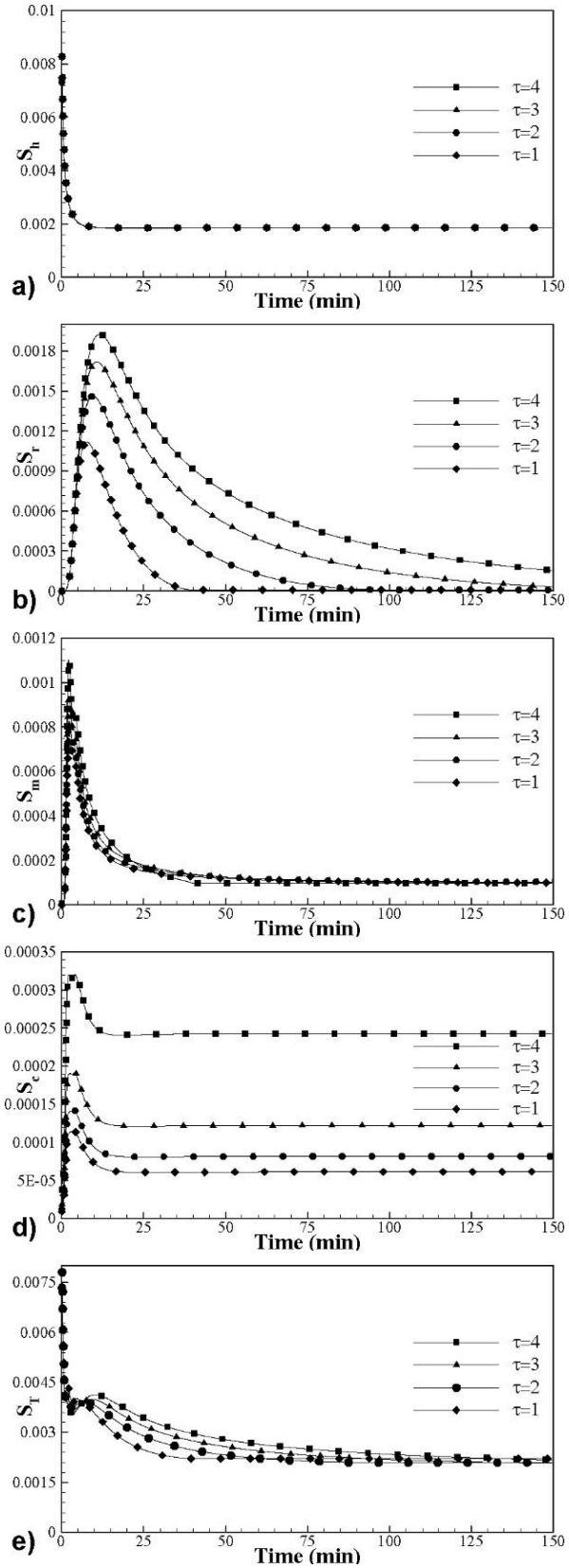

Figure 4. Entropy generation rate for different tortuosities (at $\varepsilon = 0.2, d_p = 0.01mm, GR = 1$ **)**

rate of entropy generation by heat transfer. As can be seen, tortuosity does not has a significant impact on the rate of entropy generation. Figure 4b shows the rate of entropy generation by chemical reaction. As can be seen, the rate of entropy generation increases with an increment of tortuosity. By definition, tortuosity represents a porous medium resistance against direct flow of fluid passing through it. With increasing tortuosity, the resistance of wustite pellet against gas diffusion increases and thus the rate of entropy generation increases. Figure 4c shows the rate of entropy generation by mass transfer. As can be seen, the maximum and ultimate rates of entropy generation are increased with increasing tortuosity. Figure 4d shows entropy generation by coupling between heat and mass transfer. The rate of entropy generation increases with increasing tortuosity. Figure 4e shows the rate of total entropy versus time for different tortuosities. Clearly, the rate of total entropy generation increases with an increment of tortuosity.

Figure 5 shows the entropy generation rate versus time for various ratios of reducing gases and different mechanisms of entropy generation. Figure 5a shows the rate of thermal entropy generation for different gas ratios. As can be seen, the change in the ratio of reducing gases has a little impact on the rate of thermal entropy generation. Figure 5b shows entropy generated by chemical reaction. With increasing gas ratio (the ratio of hydrogen to carbon monoxide), the rate of entropy generation decreases due to the complex relationship between the chemical potential and the rate of reaction which is dependent on the temperature and mole fraction. Figure 5c shows the rate of entropy generation versus time for various gas ratios. Increasing the gas ratio, i.e. increasing the amount of hydrogen in reducing gas led to a decrease in maximum entropy generation by mass transfer.

This can be attributed to the high diffusivity of hydrogen so that by increasing the amount of hydrogen, the transport rate of the reducing gas increases. As a result, mass gradient is reduced leading to reducing entropy generation. Figure 5d shows the impact of gas ratio on the rate of entropy generation by coupling between heat and mass transfer. As can be seen, the maximum entropy generation decreases with increasing the gas ratio due to reduced thermal and mass gradients. Figure 5e shows the rate of total entropy generation versus time for different gas ratios. By increasing the amount of hydrogen in the gas mixture, entropy generation is first decreased and then experiences a peak and finally approaches a constant value with a moderate slope.

Figure 6 shows the rate of entropy generation versus time for various grain sizes of wustite pellet and different mechanisms of entropy generation. Figure 6a shows the rate of thermal entropy generation for various

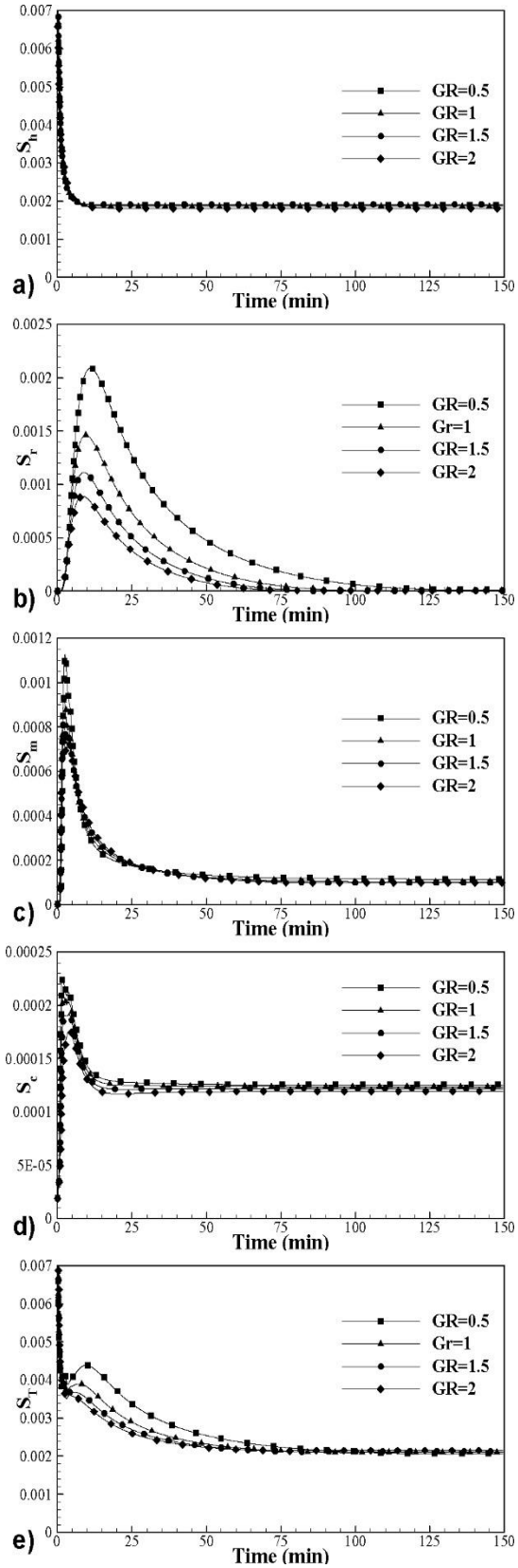

Figure 5. Entropy generation rate for different Gas ratios (at $\varepsilon = 0.2, d_p = 0.01mm, \tau = 2$)

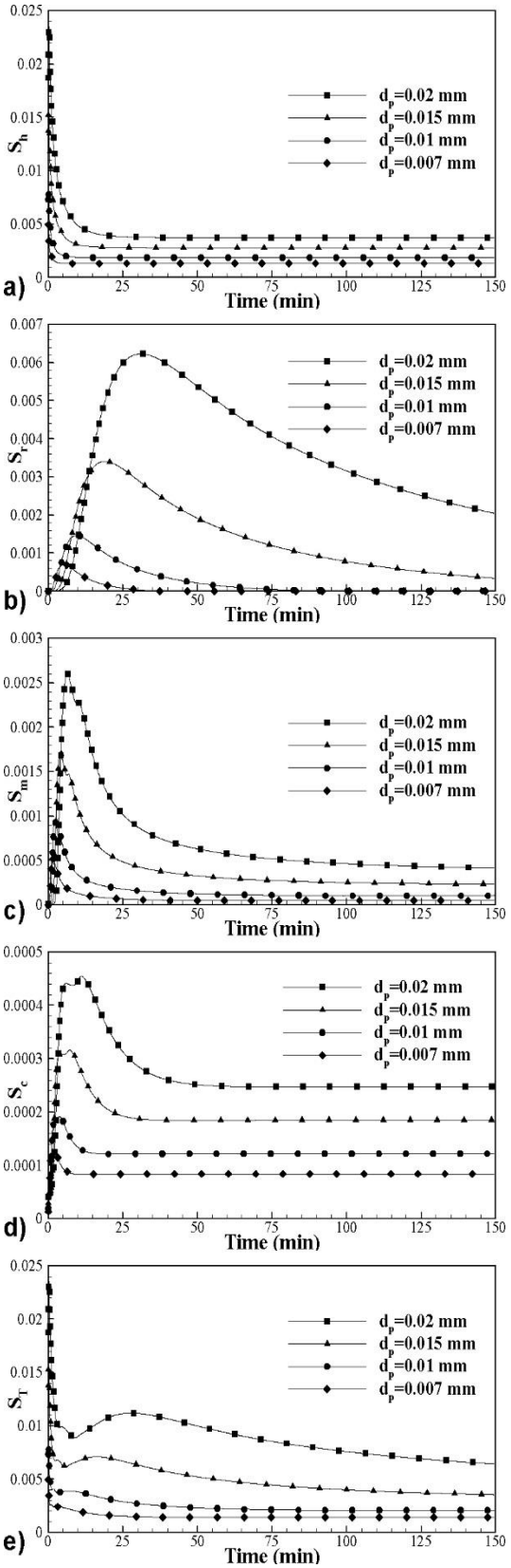

Figure 6. Entropy generation rate for different grain sizes (at $\varepsilon = 0.2, \tau = 2, GR = 1$)

grain sizes. The rate of entropy generation is highfor large grains. This means that temperature gradient is larger for larger pellets leading to increased entropy generation. Figure 6b shows the rate of entropy generation by chemical reaction. As can be seen, increasing diameter of grains is directly related to augmentation of rate of entropy generation. Figure 6c shows the rate of mass entropy generation for different grain diameters. The rate of entropy generation increases with increasing diameter. Large grains cause a significant mass gradient in the pellet being reduced. Figure 6d shows the rate of entropy generation by coupling between heat and mass transfer. This figure indicates a direct relationship between the grain size and the rate of entropy generation. Figure 6e shows the rate of total entropy generation. As can be seen, the rate of entropy generation increases with increasing grain size. Entropy first reaches a minimum value and then increases to reach a peak and finally decreases with a moderate slope.

5. CONCLUSIONS

The rate of entropy generation per unit volume of wustite pellets versus time was examined. The grain model was selected as a conceptual model to determine the reaction rate. Entropy is generated by heat transfer, mass transfer and chemical reaction. The range of porosity, totuosity, grain size and gas ratio is between 0.2 to 0.5, 1 to 4, 7 to 20 mm and 0.5 to 2, repectively. The rate of entropy generation is studied over a period of 150 minutes. The results obtained in this study can be summarized as follows:

- Maximum value of entropy generation nearly occurs during first 20 minutes of the reduction process.
- Heat transfer and coupling between heat and mass transfer had the highest and lowest contribution to entropy generation, respectively.
- The rate of thermal entropy generation sharply decreased and approached a constant value between 0.002 to 0.004 W/m^3K after about 5 minutes due to the temperature gradient in the pellet even after complete reduction. The mass entropy generation rate experienced a peak during the first 5 minutes due to the mass of reducing gas within the pellet. Finally, entropy generation reached to a constant value due to a constant mass gradient in the reduced pellet.
- Gas diffusion within the wustite pellet was facilitated with increasing porosity, leading to a decrease in the rate of entropy generation. For example when porosity increases from 0.2 to 0.5 the peak piont of entropy generation due to chemical reaction decreases from 0.0015 to 0.0006 W/m^3K.
- The resistance of porous pellet against reducing gases increased with increasing tortuosity leading to an increase in the rate of entropy generation. The highest effect of tourtousity variations is on enetropy generated by chemical reaction.
- With increasing the ratio of reducing gas, i.e. the mole fraction of hydrogen, the diffusivity of reducing gas increased leading to a decrease in the rate of entropy generation.
- The rate of entropy generation increased with increasing size of grains due to resistance to fluid penetration.

6. REFERENCES

1. Valipour, M. and Mokhtari, M., "Effect of water gas shift reaction on the non-isothermal reduction of wustite porous pellet using syngas", ***International Journal of Iron & Steel Society of Iran***, Vol. 8, No. 2, (2011), 9-15.
2. von Bogdandy, L. and Engell, H.-J., "The reduction of iron ores: Scientific basis and technology, Springer Science & Business Media, (2013).
3. McKewan, W., "Influence movement during high pressure reaction of hematite by hydrogen", ***J. Metals***, Vol. 16, No., (1964), 781-802.
4. Turkdogan, E. and Vinters, J., "Gaseous reduction of iron oxides: Part i. Reduction of hematite in hydrogen", ***Metallurgical and Materials Transactions B***, Vol. 2, No. 11, (1971), 3175-3188.
5. Usui, T., Ohmi, M. and Yamamura, E., "Analysis of rate of hydrogen reduction of porous wustite pellets basing on zone-reaction models", ***ISIJ International***, Vol. 30, No. 5, (1990), 347-355.
6. Valipour, M. and Khoshandam, B., "Numerical modelling of non-isothermal reduction of porous wustite pellet with syngas", ***Ironmaking & Steelmaking***, Vol. 36, No. 2, (2009), 91-96.
7. Ghadi, A.Z., Valipour, M.S. and Biglari, M., "Mathematical modelling of wustite pellet reduction: Grain model in comparison with uscm", ***Ironmaking & Steelmaking***, Vol. 43, No. 6, (2016), 418-425.
8. Ghadi, A.Z., Valipour, M.S. and Biglari, M., "Numerical analysis of complicated heat and mass transfer inside a wustite pellet during reducing to sponge iron by H_2 and CO gaseous mixture", ***Journal of Iron and Steel Research, International***, Vol. 23, No. 11, (2016), 1142-1150.
9. Szekely, J., "Gas-solid reactions, Elsevier, (2012).
10. Valipour, M.S. and Saboohi, Y., "Modeling of multiple noncatalytic gas–solid reactions in a moving bed of porous pellets based on finite volume method", ***Heat and Mass Transfer***, Vol. 43, No. 9, (2007), 881-894.
11. Hirschfelder, J.O., Curtiss, C.F., Bird, R.B. and Mayer, M.G., "Molecular theory of gases and liquids, Wiley New York, Vol. 26, (1954).
12. Bejan, A., "Advanced engineering thermodynamics, John Wiley & Sons, (2016).
13. Bejan, A., "Second law analysis in heat transfer", ***Energy***, Vol. 5, No. 8-9, (1980), 720-732.

14. Bejan, A., "Entropy generation through heat and fluid flow, Wiley, (1982).
15. Bejan, A., "The thermodynamic design of heat and mass transfer processes and devices", ***International Journal of Heat and Fluid Flow***, Vol. 8, No. 4, (1987), 258-276.
16. San, J., Worek, W. and Lavan, Z., "Entropy generation in convective heat transfer and isothermal convective mass transfer", ***Journal of Heat transfer***, Vol. 109, No. 3, (1987), 647-652.
17. Arpaci, V.S. and Selamet, A., "Entropy production in flames", ***Combustion and flame***, Vol. 73, No. 3, (1988), 251-259.
18. Shamsi, M. and Nassab, S.G., "Ivestigation of entropy generation in 3-d laminar forced convection flow over a backward facing step with bleeding", ***International Journal of Engineering-Transactions A: Basics***, Vol. 25, No. 4, (2012), 379-388.
19. Ziapour, B. and Rahimi, F., "Numerical study of natural convection heat transfer in a horizontal wavy absorber solar collector based on the second law analysis", ***International Journal of Engineering-Transactions A: Basics***, Vol. 29, No. 1, (2016), 109-117.
20. Dash, S. and Som, S., "Transport processes and associated irreversibilities in droplet combustion in a convective medium", ***International Journal of Energy Research***, Vol. 15, No. 7, (1991), 603-619.
21. Puri, I.K., "Second law analysis of convective droplet burning", ***International journal of heat and mass transfer***, Vol. 35, No. 10, (1992), 2571-2578.
22. Hiwase, S., Datta, A. and Som, S., "Entropy balance and exergy analysis of the process of droplet combustion", ***Journal of Physics D: Applied Physics***, Vol. 31, No. 13, (1998), 1601-1610.
23. Pope, D.N., Raghavan, V. and Gogos, G., "Gas-phase entropy generation during transient methanol droplet combustion", ***International Journal of Thermal Sciences***, Vol. 49, No. 7, (2010), 1288-1302.
24. DeHoff, R., "Thermodynamics in materials science", CRC Press, (2006).
25. Versteeg, H.K. and Malalasekera, W., "An introduction to computational fluid dynamics: The finite volume method, Pearson Education", (2007).
26. Valipour, M., "Mathematical modeling of a non-catalytic gas-solid reaction: Hematite pellet reduction with syngas", ***Scientia Iranica. Transaction C, Chemistry, Chemical Engineering***, Vol. 16, No. 2, (2009), 108-124.

Transient Entropy Generation Analysis During Wustite Pellet Reduction to Sponge Iron

A. Zare Ghadi, M. S. Valipour, M. Biglari

Faculty of Mechanical Engineering, Semnan University, Semnan, Iran

P A P E R I N F O

Paper history:
Received 28 July 2017
Received in revised form 01 December 2017
Accepted 23 January 2018

Keywords:
Wustite Pellet
Entropy Generation
Mathematical Model
Grain Model

چکیده

در کار حاضر تولید آنتروپی در طول فرایند احیای گندله وستیتی به آهن اسفنجی مورد مطالعه قرار گرفته است. روش حجم محدود برای حل معادلات حاکم استفاده شده است. مدل دانه‌ای برای شبیه‌سازی نرخ واکنش مورد استفاده قرار گرفته است. پس از اتمام فرایند احیای وستیت گازهای احیا شامل مونوکسیدکربن و هیدروژن به آب و دی کسیدکربن تبدیل می‌شوند. آنتروپی از طریق انتقال حرارت، انتقال جرم و واکنش‌های شیمیایی تولید می‌شود. نرخ تولید آنتروپی در طول زمان 150 دقیقه بررسی می‌شود. بر اساس معادلات حاکم، سهم هر فرایند در تولید آنتروپی محاسبه شده است. تاثیرات نسبت گاز، تورچیاسیتی و قطر دانه وستیتی بر روی تولید آنتروپی بررسی شده است. تخلخل در بازه 0/2 تا 0/5، تورچیاسیتی در بازه 1 تا 4، قطر ذرات در بازه 7 تا 20 میلیمتر و نسبت گاز در بازه 0/5 تا 2 متغیر است. بر طبق نتایج بیشینه مقدار تولید آنتروپی تقریبا در 20 دقیقه ابتدایی رخ می‌دهد. مشاهده شده است که انتقال حرارت بیشترین سهم در تولید آنتروپی را دارد. همچنین نتایج نشان می‌دهند، تخلخل و نسبت گاز رابطه عکس با نرخ تولید آنتروپی دارد در حالیکه تورچیاسیتی و قطر دانه با نرخ تولید آنتروپی رابطه مستقیم دارد.

***doi**: 10.5829/ije.2018.31.08b.16*